Application of statistical narrowband model to three-dimensional absorbing-emitting-scattering media
Liu, F.; Smallwood, G.J.; Gulder, O.L.

National Research Council Canada   Conseil national de recherches Canada

Canada

Application of Statistical Narrowband Model to Three-Dimensional Absorbing-Emitting-Scattering Media

Fengshan Liu,* Gregory J. Smallwood,† and Ömer L. Gülder‡
National Research Council, Ottawa, Ontario K1A 0R6, Canada

A novel method for implementing the statistical narrowband model into the radiative transfer equation was devised to perform nongrey radiative transfer calculations in three-dimensional absorbing, emitting, and scattering media. In this new method the radiation intensity is split into two parts: the nonscattered part and the scattered part. The nonscattered part is solved accurately using the statistical narrowband model and a ray-tracing technique and does not require iteration. The scattered part is solved with approximation by using the gray-band model to estimate the band correlation between the scattered intensity and the gas absorption coefficient. The accuracy of this method for narrowband radiation intensity prediction was evaluated in a homogeneous H_2O-N_2-Al_2O_3 mixture under both isothermal and nonisothermal conditions by comparing its results with those of the statistical narrowband correlated-K method. This new implementation method alleviates to some extent the difficulty of the band model-scattering incompatibility and offers good results provided the particle loading is not too high.

Nomenclature

f = species molar fraction
$I_{n\nu}$ = nonscattered part of spectral radiation intensity, W m^{-2} cm sr^{-1}
$I_{s\nu}$ = scattered part of spectral radiation intensity, W m^{-2} cm sr^{-1}
I_ν = spectral radiation intensity, W m^{-2} cm sr^{-1}
$\bar{I}_\nu$ = mean radiation intensity over a narrowband, W m^{-2} cm sr^{-1}
$k_{j\nu}$ = absorption coefficient associated with the jth quadrature point, m^{-1}
$\bar{k}_\nu$ = mean line intensity to spacing ratio, cm^{-1} atm^{-1}
L = path length, m
l_m = local mean path length, m
n = particle number density, m^{-3}
$\boldsymbol{n}$ = unit normal vector of a wall surface pointing toward the gas side
p = pressure, atm
S = surface area of a computational grid, m^2
s, s' = position variables along a line of sight, m
T = temperature, K
V = volume of a computational grid, m^3
$w_{j\nu}$ = weight parameter associated with the jth quadrature point
x, y, z = Cartesian coordinates, m
$\bar{\beta}_\nu$ = mean line width to spacing ratio
$\bar{\gamma}_\nu$ = mean half width of an absorption line, cm^{-1}
$\Delta \nu$ = wave-number interval of a narrowband, cm^{-1}
$\bar{\delta}_\nu$ = equivalent line spacing, cm^{-1}
ϵ_w = wall surface emissivity
$\kappa_{g\nu}$ = gas spectral absorption coefficient, m^{-1}
$\bar{\kappa}_{g\nu}$ = narrowband averaged gas absorption coefficient, m^{-1}

$\kappa_{p\nu}$ = particulate spectral absorption coefficient, m^{-1}
$\kappa_{s\nu}$ = particulate spectral scattering coefficient, m^{-1}
ν = wave number, cm^{-1}
ξ, η, μ = direction cosines
$\upsilon_{g\nu}$ = gas spectral transmissivity
$\upsilon_{h\nu}$ = medium spectral transmissivity associated with $I_{n\nu}$
Φ = scattering phase function
Ω = solid angle, sr
$\boldsymbol{\Omega}$ = direction of radiation propagation

Subscripts

b = blackbody
g = gas
i = spatial discretization (along a line of sight) index
n = angular discretization index
p = particulate
w = wall
ν = spectral

I. Introduction

EXTENSIVE research attention has been paid to develop accurate yet computationally efficient nongrey gas radiation models in recent years because of the important role of gas radiation in many combustion-related sciences and technologies. These models include the spectral line based weighted-sum-of-grey-gases (WSGG) model developed by Denison and Webb,[1-3] the exponential wide-band model,[4,5] the statistical narrowband (SNB) model,[5-7] and various K-distribution based methods.[8-12] As far as total (spectrally integrated) quantities are concerned, the spectral line based WSGG model of Denison and Webb, the exponential wide-band model, and correlated-K (CK) based wide-band models[9,10] offer both accuracy and computational efficiency. However, these models do not provide adequate spectral information for certain applications where low-resolution (at a resolution of 5–25 cm^{-1} bandwidth) spectral intensities are required instead of total quantities. One example of such applications is the prediction of infrared signature from a rocket plume, which is a nonisothermal mixture of radiating gases (mainly CO_2 and H_2O) and particles (soot and Al_2O_3). Although the line-by-line (LBL) method provides the exact results, its application to three-dimensional scattering problems is computationally infeasible at the present time. Therefore, approximate methods have to be developed for these applications. The SNB model is naturally a good candidate because it provides the required spectral resolution. However, the SNB model suffers from two major drawbacks. First, the straightforward implementation of the SNB model into the

radiative transfer equation (RTE) leads to complicated correlation terms,[5] and the solution of the resultant equation requires a ray-tracing technique in multidimensions.[7] These two factors dramatically increase the computing efforts of the SNB model calculations. Secondly, it encounters the so-called band model-scattering incompatibility when applied to scattering media.[13,14] The incompatibility constitutes the major obstacle to the application of the SNB model to multidimensional scattering problems.

To overcome the difficulties of the SNB model, Kim and Song[15] applied the WSGG concept to a narrowband (WNB) to maintain the compatibility of the WSGG model with the RTE in the standard form as well as the spectral resolution of the SNB model. More recently, Yang and Song[16] presented an improved version of the WNB model for CO_2 using the scaling approximation of the CK method.[17] The CK-based WNB (CKWNB) model of Yang and Song[16] is conceptually very similar to the statistical narrowband CK (SNBCK) method described by Lacis and Oinas[12] except for how the gas absorption coefficients are obtained. These two methods represent an alternative approach for low-resolution spectral intensity prediction. The SNBCK method extracts gas absorption coefficients from band-averaged gas transmissivity using inverse Laplace transformation[12] and is also a narrowband WSGG method. The advantage of the SNBCK method is that the efficient and popular discrete-ordinates method (DOM) can be used to solve the transfer equation. The seven-point Gauss–Labatto quadrature is commonly used to obtain band-averaged quantities,[8,16] which is equivalent to using seven gray gases at each narrowband; therefore, the RTE has to be solved seven times in each nonoverlapping narrowband. Hence the application of these models could also be quite time-consuming for scattering problems where solutions have to be obtained iteratively for each gray gas. At an overlapping band, which arises for radiative transfer in a mixture containing two radiating gases such as CO_2 and H_2O, the radiative transfer has to be represented by 7×7 (49) gray gases,[12] assuming each gas component is represented by seven gray gases, because the product of two Malkmus bands is no longer a Malkmus band. This quadratic increase in the number of gray gases at overlapping bands constitutes the disadvantage of the SNBCK method for overlapping band calculations.

The most simple implementation method of the SNB model is the gray narrowband model of Kim et al.[5] and Liu et al.[18] in which only one gray gas is used in each narrowband. Although the gray narrowband model of Liu et al.[18] in general offers much better results than the version of Kim et al.,[5] it predicts unreliable narrowband radiation intensities in some spectral regions in nonisothermal CO_2-H_2O gas mixtures.[19] Extension of the gray-band model to include radiation scattering is straightforward and has been done by Liu et al.[20] Through an evaluation study they found that the inclusion of scattering to the gray-band gas radiation model does not introduce extra errors.[20] This is indeed expected because the radiative properties of particulate are weakly dependent on wave number in a narrowband of 25 cm^{-1} width and can be treated as constants.

The present study made an attempt to alleviate the band model-scattering incompatibility by devising a variable splitting technique to implement the SNB model into the RTE in three-dimensional scattering media. Because benchmark narrowband results in three-dimensional scattering media are typically lacking in the literature, the accuracy of this method was evaluated by comparing its results with those obtained using the SNBCK method in a homogeneous H_2O-N_2-Al_2O_3 mixture under both isothermal and nonisothermal conditions. This mixture contains only a single radiating gas and is chosen to avoid the difficulty of the SNBCK method for calculations at overlapping bands.

II. Formulation

The spectral radiative transfer equation in absorbing, emitting, and scattering media can be written as

$$\frac{\partial I_v}{\partial s} = -(\kappa_{gv} + \kappa_{pv} + \kappa_{sv})I_v + (\kappa_{gv} + \kappa_{pv})I_{bv} + \frac{\kappa_{sv}}{4\pi}\int_{4\pi} I_v \Phi_v \, d\Omega \tag{1}$$

The corresponding boundary condition at a diffuse wall is given as

$$I_{v,w} = \epsilon_{v,w}I_{bv,w} + \frac{1 - \epsilon_{v,w}}{\pi}\int_{n\cdot\Omega<0} I_{v,w}|\xi|\, d\Omega, \quad \text{for} \quad \boldsymbol{n}\cdot\boldsymbol{\Omega} > 0 \tag{2}$$

The formal solution of Eq. (1) is[21]

$$I_v(s) = I_v(s_w)\upsilon_v(s_w \to s) + \int_{s_w}^{s} S_v(s')\upsilon(s' \to s)\, ds' \tag{3}$$

where υ_v is the spectral medium transmissivity given as

$$\upsilon_v(s_1 \to s_2) = \exp\left[-\int_{s_1}^{s_2}(\kappa_{gv} + \kappa_{pv} + \kappa_{sv})\, ds\right] \tag{4}$$

and S_v is the source function defined as

$$S_v(s) = (\kappa_{gv} + \kappa_{pv})I_{bv} + \frac{\kappa_{sv}}{4\pi}\int_{4\pi} I_v \Phi_v \, d\Omega \tag{5}$$

The direct implementation of the statistical narrowband model requires Eq. (1) to be averaged over a narrowband. This procedure results in several correlation terms. The one that deserves special attention is the correlation between the radiation intensity and the gas absorption coefficient $\overline{\kappa_{gv}I_v}$. For radiative transfer in nonscattering media, a closed form of $\overline{\kappa_{gv}I_v}$ is obtained by using Eq. (3) (Ref. 5). However, such a closed expression for $\overline{\kappa_{gv}I_v}$ no longer exists because of the dependence of I_v in Eq. (3) on the entire radiation field through the in-scattering term [the integral term on the right hand side of Eq. (5)]. This difficulty of applying a narrowband model to scattering problems was termed *band model-scattering incompatibility* by Reed et al.[14] The incompatibility is inherent for scattering problems when using the band model methodology and cannot be eliminated.

To alleviate the incompatibility of using a narrowband model to scattering problems, an alternative method to implement the SNB model into Eq. (1) is suggested in the present study. This alternative method makes use of the linear property of Eq. (1) by splitting the radiation intensity into two parts: I_{nv} and I_{sv}, representing respectively nonscattered radiation and scattered radiation,

$$I_v = I_{nv} + I_{sv} \tag{6}$$

The nonscattered part I_{nv} is set to satisfy the following transfer equation:

$$\frac{\partial I_{nv}}{\partial s} = -(\kappa_{gv} + \kappa_{pv})I_{nv} + (\kappa_{gv} + \kappa_{pv})I_{bv} \tag{7}$$

and its boundary condition is

$$I_{nv,w} = \epsilon_{v,w}I_{bv,w} \tag{8}$$

The scattered part I_{sv} has then to satisfy

$$\frac{\partial I_{sv}}{\partial s} = -(\kappa_{gv} + \kappa_{pv} + \kappa_{sv})I_{sv} - \kappa_{sv}I_{nv}$$

$$+ \frac{\kappa_{sv}}{4\pi}\int_{4\pi} I_{nv}\Phi_v \, d\Omega + \frac{\kappa_{sv}}{4\pi}\int_{4\pi} I_{sv}\Phi_v \, d\Omega \tag{9}$$

and its boundary condition is

$$I_{sv,w} = \frac{1 - \epsilon_{v,w}}{\pi}\int_{n\cdot\Omega<0}(I_{nv,w} + I_{sv,w})|\xi|\, d\Omega, \quad \text{for} \quad \boldsymbol{n}\cdot\boldsymbol{\Omega} > 0 \tag{10}$$

The presence of the nonscattered part of the intensity I_{nv} in Eqs. (9) and (10) represents the coupling between the scattered intensity and the nonscattered intensity. The scattered part I_{sv} is in general negative as a result of using this splitting scheme.

Based on the facts that the blackbody function and the radiative properties of particulate are weakly dependent on wave number in

a narrowband, the average of Eqs. (7) and (9) over a narrowband leads to

$$\frac{\partial \bar{I}_{nv}}{\partial s} = -\overline{(\kappa_{gv} + \kappa_{pv})I_{nv}} + (\bar{\kappa}_{gv} + \bar{\kappa}_{pv})\bar{I}_{bv} \quad (11)$$

$$\frac{\partial \bar{I}_{sv}}{\partial s} = -(\bar{\kappa}_{pv} + \bar{\kappa}_{sv})\bar{I}_{sv} - \overline{\kappa_{gv}I_{sv}} - \bar{\kappa}_{sv}\bar{I}_{nv}$$

$$+ \frac{\bar{\kappa}_{sv}}{4\pi}\int_{4\pi}\bar{I}_{nv}\bar{\Phi}_v\,\mathrm{d}\Omega + \frac{\bar{\kappa}_{sv}}{4\pi}\int_{4\pi}\bar{I}_{sv}\bar{\Phi}_v\,\mathrm{d}\Omega \quad (12)$$

Equation (11) can be solved rigorously without approximation by using the SNB model in the same way as that for gas radiation described by Kim et al.[5] The only modification required is to replace the gas transmissivity by the following transmissivity:

$$\bar{\upsilon}_{nv}(s_1 \to s_2) = \bar{\upsilon}_{gv}(s_1 \to s_2)\exp\left(-\int_{s_1}^{s_2}\bar{\kappa}_{pv}\,\mathrm{d}s\right) \quad (13)$$

to account for the contribution by particulate absorption and emission. Following Kim et al.,[5] the discretized form of Eq. (11) along a line of sight is written as

$$\bar{I}_{v,i+1} = \bar{I}_{v,i} + (1 - \bar{\upsilon}_{nv,i \to i+1})\bar{I}_{bv,i+\frac{1}{2}} + \bar{C}_{v,i+\frac{1}{2}} \quad (14)$$

where

$$\bar{C}_{v,i+\frac{1}{2}} = \bar{I}_{wv,1}(\bar{\upsilon}_{nv,1 \to i+1} - \bar{\upsilon}_{nv,1 \to i})$$

$$+ \sum_{k=1}^{i-1}\left[(\bar{\upsilon}_{nv,k+1 \to i+1} - \bar{\upsilon}_{nv,k+1 \to i})\right.$$

$$\left. - (\bar{\upsilon}_{nv,k \to i+1} - \bar{\upsilon}_{nv,k \to i})\right]\bar{I}_{bv,k+\frac{1}{2}} \quad (15)$$

which arises from the correlation of the sum of spectral gas absorption coefficient and particulate absorption coefficient and the nonscattered radiation intensity. The spatial discretization index $i = 1$ corresponds to the starting point of the line of sight under consideration on a wall boundary. A simpler form of the discretized RTE along a line of sight can be obtained by starting from the integral form, rather than the differential form, of the RTE. The boundary condition associated with Eq. (11) is

$$\bar{I}_{nv,w} = \epsilon_{v,w}\bar{I}_{bv,w} \quad (16)$$

Equation (12) has to be solved approximately because there is no closed form for the correlation term between the gas absorption coefficient and the scattered radiation intensity $\overline{\kappa_{gv}I_{sv}}$. The gray-band model developed by Liu et al.[18] was used to approximate this term as

$$\overline{\kappa_{gv}I_{sv}} = \bar{\kappa}_{gv}\bar{I}_{sv} \quad (17)$$

with the mean gas absorption coefficient estimated from

$$\bar{\kappa}_{gv} = -\frac{\ell n\,\bar{\upsilon}_{gv}(l_m)}{l_m} \quad (18)$$

where $l_m = 3.6$ V/S is the mean path length of the local computational control volume.[22] Using the gray-band approximation, Eq. (12) then takes a similar form as the standard RTE written in terms of absorption and scattering coefficients. Note that terms involving $\bar{I}_{nv}$ in Eq. (12) are treated as source terms because they are known once Eq. (11) is solved. Therefore, Eq. (12) can be solved by using an arbitrary solution method developed in the literature. In this work the popular discrete ordinates method was used to solve Eq. (12). The boundary condition for the band-averaged scattered radiation intensity is given as

$$\bar{I}_{sv,w} = \frac{1 - \epsilon_{v,w}}{\pi}\int_{n\cdot\Omega<0}(\bar{I}_{nv,w} + \bar{I}_{sv,w})|\xi|\,\mathrm{d}\Omega, \quad \text{for} \quad n\cdot\Omega > 0 \quad (19)$$

Although other splitting schemes of I_v are possible, the splitting just discussed offers at least two major advantages. First, solution of the nonscattered part is noniterative because it is decoupled from the scattered part and its boundary condition is in general known. Therefore, the computationally intensive ray-tracing procedure described by Liu[7] can be used to solve Eq. (14). Second, the nonscattered part I_{nv}, which is in general greater in magnitude than the scattered part, is calculated accurately. The role of radiation scattering is to redistribute but not to alter the radiant energy. Therefore, the approximation made to the correlation term in Eq. (17) to close the transfer equation of the scattered portion of the radiation intensity is therefore unlikely to reduce significantly the overall accuracy of the present method provided that the scattered part is relatively small compared to the nonscattered part. In addition, the implementation of the variable splitting strategy just discussed is not restricted to models (SNB, SNBCK) and solvers (ray-tracing, DOM) used in the present study. It allows the nonscattered part to be solved more accurately with a less accurate treatment for the scattered part.

The SNB model was used in the present study to calculate the narrowband averaged gas transmissivities. In this model the narrowband averaged transmissivity for an isothermal and homogeneous path $|s' \to s|$ is given as[23]

$$\bar{\upsilon}_{gv}(s' \to s) = \exp\left[-\frac{\bar{\beta}_v}{\pi}\left(\sqrt{1 + \frac{2\pi f p|s' \to s|\bar{k}_v}{\bar{\beta}_v}} - 1\right)\right] \quad (20)$$

where the average line width to spacing ratio is given as $\bar{\beta}_v = 2\pi\bar{\gamma}_v/\bar{\delta}_v$. For a nonisothermal and/or inhomogeneous path, the Curtis–Godson approximation[17,24] is used. The updated SNB model parameters provided by Soufiani (A. Soufiani, private communication, Ottawa, 1997) were used in the calculations of this study. This data set contains SNB model parameters for CO, CO_2, and H_2O with a constant spectral interval of 25-cm^{-1} width. The covered temperature and spectral ranges are 300–2900 K and 150–9300 cm^{-1}, respectively. Further details of the updated data set were given by Soufiani and Taine.[24]

III. Results and Discussions

The calculation of the nonscattered part, Eq. (14), was conducted first without iteration. Once the nonscattered part was obtained, the scattered part was calculated with terms containing $\bar{I}_{nv}$ acting as known source terms. The transfer equation for nonscattered radiation, Eq. (14), was solved using the ray-tracing method described by Liu.[7] Ray tracing was performed at the center of each computational grid along all the directions defined by the T_4 quadrature set (128 directions). The SNB model with the updated model parameters was used to calculate the gas transmissivity. The transfer equation for scattered radiation was solved using DOM. The spatial and angular discretizations were achieved using the positive scheme and the T_4 set, respectively, for all DOM calculations conducted in this study.

The test problem is a rectangular plume of $2 \times 2 \times 8$ m. The object is to predict the infrared signature in the wave-number range between 2000 and 4000 cm^{-1} from this plume. The plume was divided into $11 \times 11 \times 40$ control volumes. A nonuniform grid was used along the length of the plume with finer grids placed around the peak temperature for the nonisothermal case described next and uniform grid was used in the other two directions. The specified spatial resolution was found to be adequate for the results presented next, i.e., further grid refinement does not alter significantly the numerical results. The radiating gas in the plume was assumed to be a mixture of $0.2H_2O + 0.8N_2$ (mole basis) at 1 atm. A single radiating gas was considered in the present calculations to avoid the time-consuming treatment of overlapping bands encountered in the SNBCK method. The assumption was also made that the plume contains uniformly distributed aluminum oxide particles with a number density of 2×10^9 m^{-3}. The diameter of these particles is uniform at 11.6 μm. In addition, these particles are assumed to be nonabsorbing and have a refractive index of $m = 1.74$. Two sets of thermal conditions were used to perform the calculations. In the first case the plume was assumed to be isothermal at 1800 K. In

the second case the gas temperature is nonuniform but symmetrical about the centerline of the plume and is specified in terms of $T = (T_c - T_e)f(r/R) + T_e$. In this equation T_c is the gas temperature along the centerline of the plume, and T_e is the exit temperature at $z = 8$ m. Inside the circular region of the cross section of the plume, the variation of gas temperature is defined by $f(r/R) = 1 - 3(r/R)^2 + 2(r/R)^3$, where r is the distance from the plume centerline and R is the radius of the circular region ($R = 1$ m). The gas temperature outside the circular region is assumed to be uniform and at the value of the exit temperature. The centerline temperature is assumed to increase linearly from 400 K at the inlet ($z = 0$) to 2400 K at $z = 0.75$ m, then decreases linearly to 800 K at the exit. The boundaries of the plume are assumed to be black and cold.

The computational conditions just described constitute a rather severe test to evaluate the accuracy of the variable splitting method for two reasons. First, the particles are assumed to be nonabsorbing with relatively large number density, conditions that will increase the single scattering albedo. Second, the nonisothermal temperature field possesses large gradients.

Radiative properties of particles were calculated using the BHMIE code based on Mie theory.[25] The scattering phase function was approximated by the Henyey–Greenstein function[26] with the asymmetry factor calculated from Mie theory. For calculations involving radiation scattering, iterations were stopped when the relative error of the solid angle integrated intensity (gray-band intensity in the gray-band model, the scattered part of the intensity in the present method, or the intensity of the jth gray gas in the SNBCK method) is less than 1×10^{-2}.

Because narrowband results in three-dimensional scattering media are not available in the open literature, at least to our knowledge, results of the variable splitting method are compared with those obtained using the SNBCK method[12] and the gray-band model.[20] Results of the SNBCK method cannot be treated as a benchmark solution because of its approximate nature. However, they serve as a good reference solution to evaluate the accuracy of the variable splitting method.

A detailed description of the SNBCK method can be found in Lacis and Oinas.[12] The RTE associated with the jth quadrature point takes the following form:

$$\frac{\partial I_{j\nu}}{\partial s} = -(k_{j\nu} + \kappa_{p\nu} + \kappa_{s\nu})I_{j\nu} + (k_{j\nu} + \kappa_{p\nu})I_{b\nu}$$

$$+ \frac{\kappa_{s\nu}}{4\pi} \int_{4\pi} I_{j\nu} \Phi_\nu \, d\Omega \qquad (21)$$

where $k_{j\nu}$ is the gas absorption coefficient at the jth quadrature point. The narrowband intensity is calculated as

$$\bar{I}_\nu = \sum_{j=1}^{7} \omega_{j\nu} I_{j\nu} \qquad (22)$$

where $\omega_{j\nu}$ is the weight parameter associated with the jth quadrature point. The seven-point Gauss–Labatto quadrature points and coefficients are given in Rivière et al.[8] The relative errors of the gas transmissivities over isothermal and homogeneous columns calculated using the seven-point Gauss–Labatto quadrature are less than 2%, compared to the transmissivities of the SNB model. The RTE of the SNBCK method, Eq. (21), was solved using DOM with the positive spatial differencing scheme.

Because the objective of the present paper is to demonstrate the accuracy and capability of the variable splitting method, numerical calculations were conducted in the spectral region of 2000 to 4000 cm^{-1} instead of the entire infrared range. To evaluate the performance of the present variable splitting method for scattering calculations, numerical calculations were first performed for the nonscattering isothermal case ($T = 1800$ K) by setting the particulate scattering coefficient to zero. Comparing the performance of the variable splitting method and the gray-band model of Liu et al.[20] for scattering problems as they bear some similarity in the treatment of the correlation term yet differ fundamentally is also interesting. In
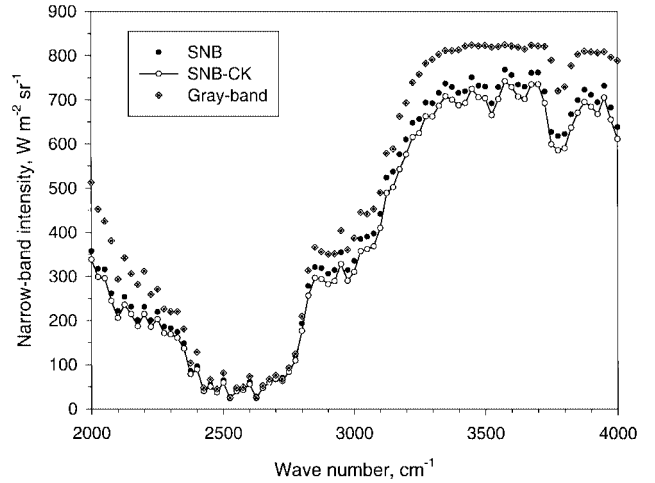

Fig. 1 Comparisons of narrowband integrated radiation intensities at (1 m, 1 m, 7.9 m) and along the direction (0.0990147, 0.0990147, 0.990147) for the isothermal case without scattering.

the gray-band model of Liu et al.,[20] the correlation between the spectral radiation intensity and the gas absorption coefficient was evaluated approximately using the noncorrelated expression, Eq. (17). As a result, this model produces significant errors in the calculations of narrowband intensities in a nonisothermal CO_2-H_2O mixture.[19] In contrast, the variable splitting method treats the gas radiation (the nonscattered part of the intensity) rigorously, which is the difficult part of the problem, and makes use of the gray-band approximation, Eqs. (17) and (18), only to the scattered part of the intensity, which is in general smaller in magnitude compared to the nonscattered part. A direct comparison of the results of the variable splitting method and the gray-band model serves to illustrate the improvement in accuracy achieved by the variable splitting strategy with the SNBCK results as a reference.

Figure 1 shows the infrared signature (narrowband integrated radiation intensity) viewed at $(x, y, z) = (1$ m, 1 m, 7.9 m) and along the direction (0.0990147, 0.0990147, 0.990147) for this isothermal and nonscattering case. This direction is the first discrete ordinate in the T_4 set and is almost in parallel with the plume centerline. Results of the SNB model are in good agreement with the results of the SNBCK method, and the difference between them is within 10%. The discrepancy between the results of these two methods is caused by using two different solvers, i.e., ray tracing for the SNB model and DOM for the SNBCK method. The ray-tracing method is numerically more accurate than DOM as far as radiation intensity along a line of sight is concerned. This is because in the ray-tracing algorithm the RTE is discretized along the direction of radiation propagation, which is one-dimensional. The gray-band results are qualitatively correct but significantly erroneous at most of the bands.

Numerical calculations were then carried out for the isothermal and scattering case, and the results are compared in Fig. 2 for infrared signature along the same line of sight as in Fig. 1. The agreement between the results of the present variable splitting method and the SNBCK method is found to be similar to and even better for some bands than what was observed in Fig. 1. This apparent improved agreement between the results of the two methods found in Fig. 2, compared to those in Fig. 1, is actually caused by the errors of the variable splitting method for scattering calculations. On the one hand, the ray-tracing algorithm for the nonscattered part tends to predict higher intensities than the SNBCK method using DOM, Fig. 1. On the other hand, the gray-band approximation used in the calculation of the scattered part in general overestimates the magnitude of the intensity based on our previous studies.[19,20] Note that the scattered part is negative in the present context. Therefore, the combined effects of using ray tracing for the nonscattered part and gray-band approximation for the scattered part lead to improved agreement between the results of the variable splitting and the SNBCK. Results shown in Figs. 1 and 2 indicate that the variable splitting method
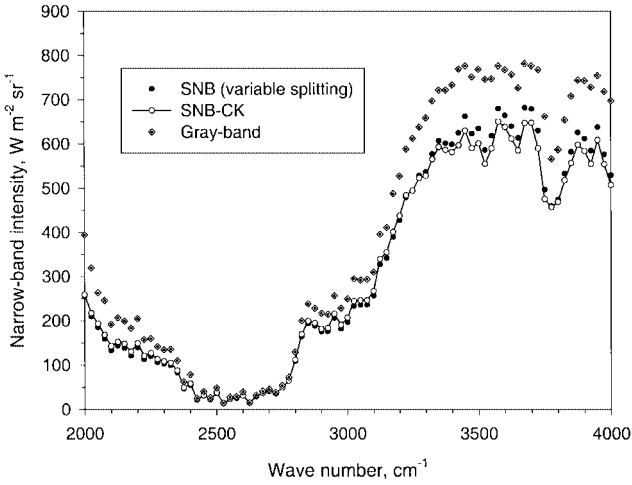
Fig. 2   Comparisons of narrowband integrated radiation intensities at (1 m, 1 m, 7.9 m) and along the direction (0.0990147, 0.0990147, 0.990147) for the isothermal case with scattering. Particle number density is 2×10^9 m^{-3}.
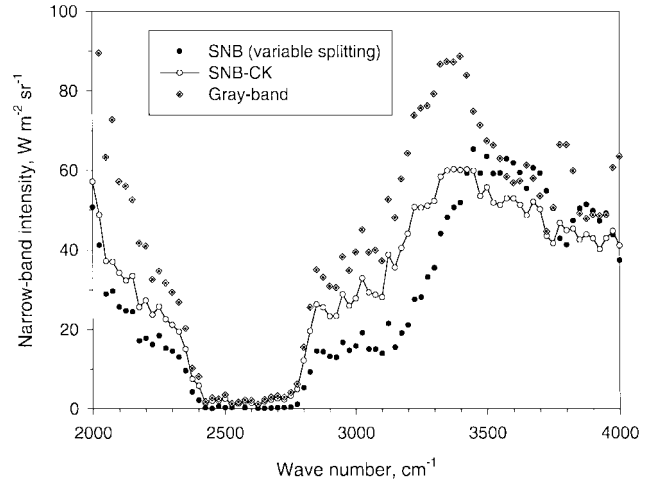

Fig. 4   Comparisons of narrowband integrated radiation intensities at (1 m, 1 m, 7.9 m) and along the direction (0.0990147, 0.0990147, 0.990147) for the nonisothermal case with scattering. Particle number density is 2×10^9 m^{-3}.
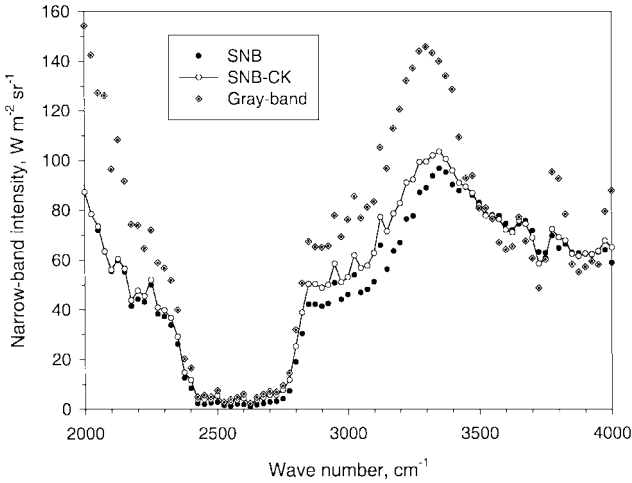

Fig. 3   Comparisons of narrowband integrated radiation intensities at (1 m, 1 m, 7.9 m) and along the direction (0.0990147, 0.0990147, 0.990147) for the nonisothermal case without scattering.
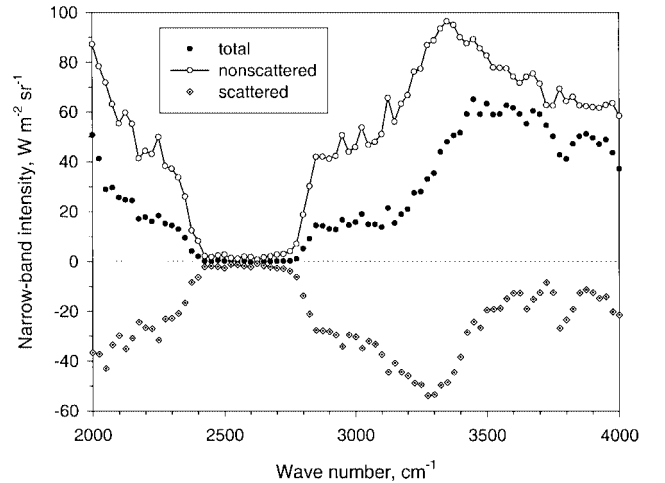

Fig. 5   Nonscattered and scattered portions of the narrowband integrated intensities at (1 m, 1 m, 7.9 m) and along the direction (0.0990147, 0.0990147, 0.990147) for the nonisothermal case with scattering. Particle number density is 2×10^9 m^{-3}.

offers similar accuracy to the SNBCK method in this isothermal scattering case. Again, results of the gray-band model are significantly erroneous as shown in the nonscattering case, Fig. 1. Comparison between results shown in Figs. 1 and 2 shows that the effect of particle scattering under these conditions is to lower radiation intensity along this line of sight.

Figure 3 shows the narrowband intensities along the line of sight defined in Fig. 1 for the nonisothermal and nonscattering case. Good agreement was found between the results of the SNB model and the SNBCK method, except in the wave-number region between 2800 and 3300 cm^{-1} where the discrepancy reaches about 30%. Part of such a large discrepancy is attributed to difference caused by using two different solvers as mentioned earlier. However, the discrepancy is mainly caused by the two different approximations made in the SNB model and the SNBCK method for nonisothermal media. The Curtis–Godson approximation was used to obtain equivalent band parameters for the calculation of gas transmissivity along a nonisothermal path[17] in the SNB model, whereas the scaling approximation was used in the SNBCK method for application to nonisothermal media.[17] The question of which model is more accurate for radiative transfer calculation in nonisothermal media can only be answered with the help of more accurate results, such as from line-by-line calculations, and is beyond the scope of the present study. Nevertheless, the results shown in Fig. 3 serve as a reference

to evaluate the performance of the variable splitting method for the nonisothermal scattering case to be shown in Fig. 4. The gray-band model yields large errors at most of the bands calculated.

Results of the nonisothermal scattering case along the same line of sight are shown in Fig. 4. A comparison between the results of the SNB and the SNBCK shown in Fig. 4 and those in Fig. 3 implies that the variable splitting method predicts unsatisfactory band-averaged intensities for this nonisothermal scattering case because the level of agreement between the results of the variable splitting and the SNBCK method in Fig. 4 deteriorates significantly compared to that in Fig. 3. The results of the variable splitting method are in general still better than the gray-band results.

As a direct consequence of variable splitting, the present method naturally separates the scattered and the nonscattered portions of the radiation intensity. The effects of scattering can be readily analyzed from the calculations using this method. For the nonisothermal and scattering case the scattered and the nonscattered portions of the narrowband intensities along the line-of-sight defined in Fig. 1 are shown in Fig. 5 along with the total (sum of the scattered and the nonscattered portions) intensities. The importance of scattering in each band are clearly seen. The scattered portion of the intensity is in general negative because in the present variable splitting scheme the transfer equation of the scattered part, Eq. (9), contains all terms

Table 1   CPU times (s) of the three methods in the calculations of the three scattering cases

Run conditions	Gray-band	SNB (variable splitting)	SNBCK
Isothermal, $n = 2 \times 10^9$ m^{-3}	8,019.6	61,242.7	75,481.8
Nonisothermal, $n = 2 \times 10^9$ m^{-3}	9,480.3	61,442.4	92,619.0
Nonisothermal, $n = 2 \times 10^8$ m^{-3}	4,768.5	54,938.3	48,170.2
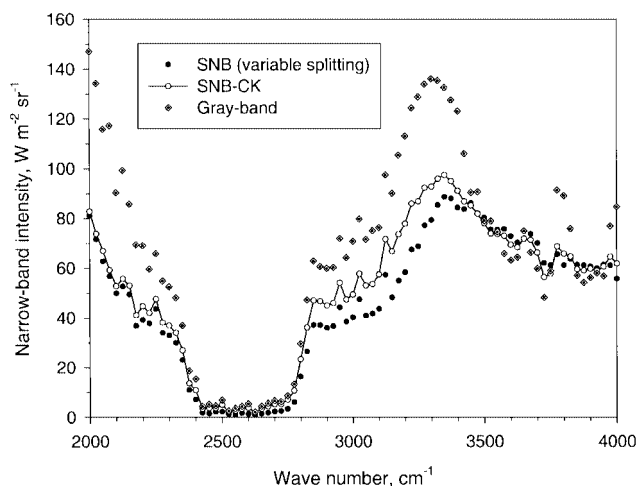
Fig. 6   Comparisons of narrowband integrated radiation intensities at (1 m, 1 m, 7.9 m) and along the direction (0.0990147, 0.0990147, 0.990147) for the nonisothermal case with scattering. Particle number density is 2×10^8 m^{-3}.
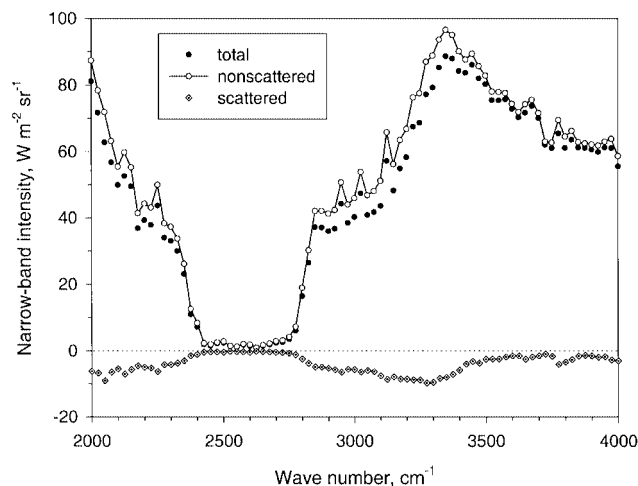
Fig. 7   Nonscattered and scattered portions of the narrowband integrated intensities at (1 m, 1 m, 7.9 m) and along the direction (0.0990147, 0.0990147, 0.990147) for the nonisothermal case with scattering. Particle number density is 2×10^8 m^{-3}.

related to scattering. To be specific, the source terms of Eq. (9) (terms containing $I_{n\nu}$) are almost always negative.

To examine the performance of the variable splitting method at lower particle number densities, numerical calculations were conducted for the nonisothermal scattering case with a particle number density of 2.0×10^8 m^{-3} and the results are compared in Fig. 6 for narrowband intensities along the same line of sight as just mentioned. The level of agreement between the results of the SNB and the SNBCK methods in Fig. 6 is seen to be similar to that observed in the nonscattering case shown in Fig. 3, indicating that the results of the variable splitting method for this lower particle loading case are quite accurate.

The relative importance of the nonscattered part and the scattered part of radiation intensity for the nonisothermal and lower particle loading case is shown in Fig. 7. The magnitude of scattered part is reduced by about a factor of four compared to the high particle loading case, Fig. 5.

All of the numerical calculations of the present study were performed on a SGI Octane at 175 MHz. The CPU times of the three scattering cases (isothermal and higher particle loading, nonisothermal and higher particle loading, and nonisothermal and lower particle loading) are compared in Table 1.

The CPU time of the gray-band model is about an order of magnitude lower than those of the other two methods. For the two higher particle loading cases the variable splitting method requires less CPU time than the SNBCK method. For the lower particle loading case, however, the variable splitting method requires slightly more CPU time. In addition, the CPU time of the variable splitting method is less affected by the level of particle loading because most of the CPU time of the variable splitting method is consumed in the calculation of the nonscattered part using the ray-tracing algorithm. The CPU times given in Table 1 were for a relatively large relative error of 1.0×10^{-2} used as the convergence criterion for the iteration and a single radiating gas calculations. Under these conditions the variable splitting method does not offer better computational efficiency than the SNBCK method. If a more stringent criterion is used in the iteration or the problem involves two or three radiating gases, which is often the situation for practical applications, the variable

splitting method will be more efficient than the SNBCK method. At an overlapping band the CPU time of the variable splitting method remains almost the same as that at a nonoverlapping band. However, the CPU time of the SNBCK method increases by about a factor of seven for an overlapping band calculation.

IV.   Conclusions

A variable splitting method was developed to incorporate the statistical narrowband model into the radiative transfer equation to calculate narrowband radiation intensities in three-dimensional absorbing, emitting, and scattering media. The method offers similar accuracy as the SNBCK method in the isothermal case. For nonisothermal gas-particle mixtures, the method offers good accuracy for low to intermediate particle loadings. However, results of the variable splitting method are inaccurate for nonisothermal and high particle loading mixtures. For problems containing a single radiating gas the variable splitting method offers similar computational efficiency to the SNBCK approach. The variable splitting method will become more efficient than the SNBCK method for problems involving two or more radiating gases. The method developed in this work alleviates to some extent the band model-scattering incompatibility difficulty of the statistical narrowband model. This study demonstrates that the statistical narrowband has a good potential in the prediction of nongray radiative transfer in three-dimensional scattering media provided that the particle loading is not too high.

Acknowledgments

References

[1] Denison, M. K., and Webb, B. W., "A Spectral Line-Based Weighted-Sum-of-Grey-Gases Model for Arbitrary RTE Solvers," *Journal of Heat Transfer*, Vol. 115, No. 4, 1993, pp. 1004–1012.

[2] Denison, M. K., and Webb, B. W., "An Absorption-Line Blackbody Distribution Function for Efficient Calculation of Total Gas Radiative Transfer,"

Journal of Quantitative Spectroscopy and Radiative Transfer, Vol. 50, No. 5, 1993, pp. 499–510.

[3]Denison, M. K., and Webb, B. W., "The Spectral Line-Based Weighted-Sum-of-Grey-Gases Model in Non-Isothermal Non-Homogeneous Media," *Journal of Heat Transfer*, Vol. 117, No. 2, 1995, pp. 339–365.

[4]Edwards, D. K., "Molecular Gas Band Radiation," *Advances in Heat Transfer*, edited by T. F. Irvine Jr. and J. P. Hartnett, Vol. 12, Academic, New York, 1976, pp. 115–193.

[5]Kim, T-K., Menart, J. A., and Lee, H. S., "Nongray Radiative Gas Analysis Using the S-N Discrete Ordinates Method," *Journal of Heat Transfer*, Vol. 113, No. 4, 1991, pp. 946–952.

[6]Zhang, L., Soufiani, A., and Taine, J., "Spectral Correlated and Non-Correlated Radiative Transfer in a Finite Axisymmetric System Containing an Absorbing and Emitting Real Gas-Particle Mixture," *International Journal of Heat Mass Transfer*, Vol. 31, No. 11, 1985, pp. 2261–2272.

[7]Liu, F., "Numerical Solutions of Three-Dimensional Non-Grey Gas Radiative Transfer Using the Statistical Narrow-Band Model," *Journal of Heat Transfer*, Vol. 121, No. 1, 1999, pp. 200–203.

[8]Rivière, P. H., Soufiani, A., and Taine, J., "Correlated-k and Fictitious Gas Methods for H_2O Near 2.7 μm," *Journal of Quantitative Spectroscopy and Radiative Transfer*, Vol. 48, No. 2, 1992, pp. 187–203.

[9]Tang, K. C., and Brewster, M. Q., "K-Distribution Analysis of Gas Radiation with Nongrey, Emitting, Absorbing, and Anisotropic Scattering Particles," *Journal of Heat Transfer*, Vol. 116, No. 4, 1994, pp. 980–985.

[10]Marin, O., and Buckius, R. O., "Wideband Correlated-k Method Applied to Absorbing, Emitting, and Scattering Media," *Journal of Thermophysics and Heat Transfer*, Vol. 10, No. 2, 1996, pp. 364–371.

[11]Lee, P. Y. C., Hollands, K. G. T., and Raithby, G. D., "Reordering the Absorption Coefficient within the Wide Band for Predicting Gaseous Radiant Exchange," *Journal of Heat Transfer*, Vol. 118, No. 2, 1996, pp. 394–400.

[12]Lacis, A. A., and Oinas, V., "A Description of the Correlated k Distribution Method for Modeling Nongray Gaseous Absorption, Thermal Emission, and Multiple Scattering in Vertically Inhomogeneous Atmosphere," *Journal of Geophysical Research*, Vol. 96, No. D5, 1991, pp. 9027–9063.

[13]Soufiani, A., "Gas Radiation Spectral Correlated Approaches for Industrial Applications," *Heat Transfer in Radiating and Combusting Systems*, edited by M. G. Carvalho, F. C. Lockwood, and J. Taine, Springer–Verlag, Berlin, 1991.

[14]Reed, R. A., Brown, D. G., Hiers, R. S., III, Cromwell, B. K., and Zaccardi, V. A., "Compatibility of Infrared Band Models with Scattering," *Journal of Thermophysics Heat Transfer*, Vol. 8, No. 2, 1994, pp. 208–215.

[15]Kim, O. J., and Song, T-H., "Implementation of the Weighted Sum of Gray Gases Model to a Narrow Band: Application and Validity," *Numerical Heat Transfer, Part B*, Vol. 30, 1996, pp. 453–468.

[16]Yang, S-S, and Song, T-H., "An Improved WSGGM-Based Narrow Band Model for CO_2 4.3 μm Band," *Revue Générale de Thermique*, Vol. 38, No. 3, 1998, pp. 228–238.

[17]Goody, R. M., and Yung, Y. L., *Atmospheric Radiation*, 2nd ed., Oxford Univ. Press, Oxford, 1989.

[18]Liu, F., Gülder, Ö. L., Smallwood, G. J., and Ju, Y., "Non-Grey Gas Radiative Transfer Analyses Using the Statistical Narrow-Band Model," *International Journal of Heat Mass Transfer*, Vol. 41, No. 14, 1998, pp. 2227–2236.

[19]Liu, F., Gülder, Ö. L., and Smallwood, G. J., "Three-Dimensional Non-Grey Gas Radiative Transfer Analyses Using the Statistical Narrow-Band Model," *Revue Générale de Thermique*, Vol. 37, No. 7, 1998, pp. 759–768.

[20]Liu, F., Gülder, Ö. L., and Smallwood, G. J., "Evaluation of an Approximate Narrow-Band Formulation for Non-Grey Radiative Transfer Calculation in Three-Dimensional Absorbing-Emitting-Scattering Media," Proceedings of the 7th AIAA/ASME Joint Thermophysics and Heat Transfer Conference, Vol. 1, American Society of Mechanical Engineers, New York, 1998, pp. 33–39.

[21]Modest, M. F., *Radiative Heat Transfer*, McGraw–Hill, New York, 1993, p. 305.

[22]Hottel, H. C., and Sarofim, A. F., *Radiative Transfer*, McGraw–Hill, New York, 1967, p. 278.

[23]Ludwig, D. B., Malkmus, W., Reardon, J. E., and Thomson, J. A. L., "Handbook of Infrared Radiation from Combustion Gases," NASA SP3080, 1973.

[24]Soufiani, A., and Taine, J., "High Temperature Gas Radiative Property Parameters of Statistical Narrow-Band Model for H_2O, CO_2 and CO, and Correlated-K Model for H_2O and CO_2," *International Journal of Heat Mass Transfer*, Vol. 40, No. 4, 1997, pp. 987–991.

[25]Bohren, C. F., and Huffman, D. R., *Absorption and Scattering of Light by Small Particles*, Wiley, New York, 1983, pp. 479–482.

[26]Viskanta, R., and Mengüc, M. P., "Radiation Heat Transfer in Combustion Systems," *Progress in Energy and Combustion Science*, Vol. 13, No. 2, 1987, pp. 97–160.